N00014-88-J-1072

ONT FINAL REPORT FOR SHARKA M. PROKES

As an ONT Postdoctoral Fellow for the past two years, I have been able to accomplish a significant amount of work in semiconductor thin films, especially GaAs on silicon heteroepitaxy. I have been involved in the growth of GaAs on silicon, and my interest has been concentrated in defect reduction and propagation. To this end, I have developed a new buffer layer technique which is formed by the implantation of germanium into silicon (100) and silicon (100) 4° to [110]. The implanted wafers are then wet oxidized and a single crystal graded SiGe layer is formed. The second step then involves the growth of GaAs on this substrate. The final GaAs/SiGe/Si heterostructures have a reduction of misfit and threading dislocations, due to better lattice matching and thermal expansion coefficients of the SiGe alloy.

The implanted substrates were examined by Auger, Rutherford Backscattering, Electroreflectance, photoluminesence, XTEM, SEM, and RED (reflected electron diffraction). Three papers have been published on this topic, with a fourth paper in progress.

Additional work has been done on GaAs/AlGaAs heterostuctures, especially defect generation and propagation. This work is ongoing and extending to superlattices of SiGe/Si and InGaAs/GaAs.

Furthermore, additional work has been done on SIMOX (silicon implanted by oxygen), in which we have examined defects by photoluminescence, electron spin resonance, and XTEM (cross-sectional transmission electron microscopy). SIMOX is another possible substrate for GaAs/Si growth, since the buried oxygen layer allows electrical isolation for radiation-hard devices. Several papers have also been published in these two areas.

Overall, my experience as an ONT post-doc has been positive, except for my initial advisor, Dr. E.D. Richmond. Dr. Richmond should not be allowed to guide any post-doctoral fellows, since he lacks the qualities of a good advisor and he is not a competent scientist (my report concerning this topic should be on file).

Since my transfer to Dr. A. Christou, I have had the freedom and the opportunity to pursue my interests in electronic materials, as is evident from the work reviewed above. I have thus chosen to stay in Dr. Christou's branch as a permanent employee.

To Published in APL Dec 21, 1988

# THE FORMATION OF EPITAXIAL $Si_{1-x}Ge_x$ FILMS PRODUCED BY WET OXIDATION OF AMORPHOUS SiGe LAYERS DEPOSITED ON SI(100)

S.M. Prokes*, W.F. Tseng, and A. Christou

Naval Research Laboratory

Washington, DC 20375

Epitaxial SiGe/Si structures have been formed by wet oxidation of amorphous SiGe films. Amorphous, 1000Å thick $Si_{0.86}Ge_{0.14}$ films were electron beam evaporated onto RCA cleaned Si(100) substrates at a background pressure of $1x10^{-7}$ torr. They were then wet oxidized in an open-tube furnace, at 900°C for various times. They have been examined by Reflective High Energy Electron Diffraction (RHEED) and Rutherford Backscattering (RBS). Results indicate the formation of an epitaxial SiGe layer following the oxidation, whereas a polycrystalline layer forms following a vacuum or nitrogen ambient anneal. It is suggested that the oxide contamination at the amorphous SiGe/Si interface is too high to allow Solid Phase Epitaxial (SPE) growth to occur in an oxygen-free ambient, but during the oxidation process, some native oxide is dissolved due to a gradient of silicon from the substrate to the growing $SiO_2$ on the surface. This allows grains of the SiGe alloy to orient with respect to the substrate, and secondary grain growth occurs during the oxidation process.

*ONT Postdoctoral Fellow

Ge-Si heterostructures are currently of interest due to their potentially useful optical and electronic properties. At this point, high quality strained SiGe/Si layers have been produced by molecular beam epitaxy (MBE) [1] or chemical vapor deposition (CVD)[2]. A technique such as MBE allows precise control on the scale of a fraction of a monolayer, thus allowing possible band structure engineering and tailoring of the transport and optical properties of this system [3]. These techniques, however, require extremely low interfacial contamination, and precise temperature control.

Investigations of the formation of epitaxial Si and Ge heterostructures by solid-phase epitaxial regrowth of evaporated amorphous films [4,5,6] have also been made. Interfacial contamination is a very important consideration in that results indicate that a very clean interface beween the Si substrate and the amorphous layer must exist before any SPE occurs. Recently, SPE of amorphous Ge layers has been achieved by Abelson et al. [7], produced by pulsed laser mixing. In this case, the Si and amorphous Ge interface is melted during the laser annealing, allowing SPE to occur.

Fathy et al. [9] have reported on the formation of an epitaxial SiGe layer following the wet oxidation of a germanium implanted silicon substrate. In this work, we demonstrate the formation of an epitaxial, germanium-rich heterostructure formed by wet oxidation of an initially amorphous SiGe alloy evaporated on Si(100). It has been found that the amount of interfacial contamination is not critical to the epitaxial layer formation, owing to the specific kinetics associated with the rapid oxidation process.

Si (100) wafers, boron-doped to 30Ω-cm, were obtained from Virginia Semiconductor. They were RCA cleaned and introduced into a standard electron-beam

evaporator, having a background pressure of $1x10^{-7}$ torr. Amorphous $Si_{0.86}Ge_{0.14}$ layers 1000Å thick were deposited directly onto Si(100) substrates at room temperature at a rate of 2Å's. No special precautions were taken to insure a clean interface. Following the deposition, the samples were cut into 2cmx2cm pieces, dipped in hot trichloroethylene, acetone, and methanol, and etched in HF for ten seconds. Sample #1 was introduced into a tube furnace, which was flushed with nitrogen, and then brought to 900°C. The sample was oxidized at 900°C in a steam ambient for 30 minutes. Samples #2 and #3 were oxidized in a similar manner, but for a time of 60 and 120 minutes, respectively.

A reflected high energy diffraction (RHEED) pattern of sample #1 is shown in Fig. 1a. The pattern exhibits a polycrystalline pattern for the SiGe layer. The RHEED pattern for sample #2 is shown in 1c and 1d. Here, the sample exhibits a dual pattern, that of a single crystal pattern superimposed onto a polycrystalline pattern. Fig. 1c shows the pattern in a [100] direction, while 1d is along a [110] direction. A distinct single crystal pattern is visible in Fig. 1e and 1f, which is the RHEED pattern for sample #3 along the [100] and [110] directions, respectively. Another sample, referred to as #4, was annealed under UHV conditions ($8x10^{-10}$ torr) for 60 minutes at 850°C. The RHEED pattern, shown in Fig. 1b, is polycrystalline. In addition, a similar sample was annealed in a nitrogen ambient in the tube furnace for 120 minutes, at 900°C. The sample was also found to be polycrystalline, using X-ray diffraction. This is a clear indication that the initial silicon/amorphous SiGe interface contains a relatively thick native oxide layer, from which SPE cannot occur under normal annealing conditions.

Rutherford backscattering has been used to examine the thickness and crystallinity of the SiGe layer of sample #3, using a 3MeV $^4He^{++}$ beam at an angle of 170°. Fig. 2 shows random and channeling spectra of sample #3. A distinct germanium-rich

layer is seen, which is about 530Å thick, as determined from Cornell University's RUMP simulation [8]. The sample also exhibits channeling, indicating a single crystal SiGe layer.

The initial amorphous layer was composed of 14% germanium, as determined by microprobe analysis. After the wet oxidation process, the germanium concentration near the thermal oxide/SiGe interface was measured to be 59%, using Raman Spectroscopy, which is described elsewhere [10].

A possible mechanism which could explain the experimental results is as follows. During the initial stages of the wet oxidation process at 900°C, the samples form fine polycrystallites, as seen in the RHEED data. As the oxidation process continues, the germanium is rejected by the thermal oxide, and piles up at the Si and SiOJ interface. As the growing oxide begins consuming the silicon in the polycrystalline layer, a silicon gradient develops which results in the diffusion of silicon from the substrate through the Ge-rich layer [9] to the growing oxide. Earlier data indicate that the diffusion of silicon through germanium can be a very rapid process [11]. This silicon diffusion causes bond breaking in the native oxide present at the amorphous SiGe/Si interface, (described as an $SiO_2$ continuous random network). As the bonds break, oxygen becomes free to form precipitates or diffuse rapidly through the silicon lattice, as has been reported by Newman et al. [12]. Thus, there will be areas of the interface where the native oxide is dissolved, which allows the polycrystalline SiGe alloy above this interface to make direct contact with the substrate silicon. Some SiGe grains then orient with respect to the (100) substrate, in the native oxide-free areas. As oxidation continues, large (100) oriented crystallites appear, which fully transform to a single crystal. Fig. 1c and 1d support this proposed mechanism, since one would expect to see oriented

crystals (RHEED spots) along with the polycrystalline pattern. As the oxidation continues further, the preferred grains grow at the expense of all others. This is referred to as secondary grain growth, and has been suggested as a possible mechanism for homoepitaxy and for growth of single crystal silicon on $SiO_2$ substrate [13].

Thus, we have formed epitaxial, SiGe thin films from an amorphous SiGe evaporated layer, by the use of wet oxidation. Samples which have been annealed in vacuum or a nitrogen ambient become polycrystalline due to the presence of a native oxide at the a-SiGe and Si interface. However, the samples produced by wet oxidation exhibit a single crystal structure.

A possible explanation is as follows. As the oxidation process proceeds, germanium piles up at the thermal oxide/SiGe interface. For the oxidation process to continue, silicon must diffuse through the germanium to form $SiO_2$. As silicon is depleted from the thin SiGe layer, a silicon gradient develops, and substrate silicon begins diffusing through the native oxide layer and the germanium, to reach the growing thermal oxide. This diffusion leads to the breaking of bonds at the native oxide/substrate interface, creating native oxide-free areas. This allows some SiGe polycrystallites to orient with respect to the (100) substrate, and to grow by secondary grain growth, as the oxidation process continues, until the whole film is single crystal.

The authors would like to thank S.S. Lau and L.C. Wang for help with the RBS, O.J. Glembocki for help with the Raman, W.E. Carlos and R. Stahlbush for helpful discussions, and R.C. Cammarata for critical reading of the manuscript.

## REFERENCES


1. J.C. Bean, L.C. Feldman, A.T. Fiory, S. Nakahara, and I.K. Robinson, J. Vac. Sci. Technol. A 2 (1984) 436.
2. C.M. Gronet, C.A. King, W. Opyd, J.F. Gibbons, S.D. Wilson, and R. Hull, J. Appl. Phys. 61 (1987) 2407.
3. J. Bevk, J.P. Mannaerts, L.C. Feldman, B.A. Davidson, and A. Ourmazd, Appl. Phys. Lett. 49 (1986) 286.
4. M. von Allmen, S.S. Lau, D.M. Scott, J.W. Mayer, W.F. Tseng, T.T. Sheng, P. Williams, and J.E. Baker, Proceedings of Symposium on Thin Film Interfaces and Interactions, Electrochemical Soc. 80(2) (1980) 195.
5. M.G. Grimaldi, M. Maenpaa, B.M. Paine, M-A. Nicolet, S.S. Lau, and W.F. Tseng, J. Appl. Phys. 52 (1981) 1351.
6. L.S. Hung, S.S. Lau, M. von Allmen, J.W. Mayer, B.M. Ulrich, J.E. Baker, P. Williams, and W.F. Tseng, Appl. Phys. Lett. 37 (1980) 909.
7. J.R. Abelson, T.W. Sigmon, Ki Bum Kim, and K.H. Weiner, Appl. Phys. Lett. 52 (1988) 230.
8. L.R. Doolittle, Nucl. Instr. and Meth. B9 (1983) 344.
9. D. Fathy, O.W. Holland, and C.W. White, Appl. Phys. Lett. 51 (1987) 1337.
10. S.M. Prokes, O.J. Glembocki, E.P. Donovan, R. Stahlbush, W.E. Carlos, H. Dietrich and A. Christou, SPIE Proceedings, Newport Beach, CA (1988), to be published.
11. S.M. Prokes and F. Spaepen, Appl. Phys. Lett. 47 (1985) 234.
12. R.C. Newman, M.J. Binns, W.P. Brown, F.M. Livingston, S. Messoloras, R.J. Stewart, and J.G. Wilkes, Physica 116B (1983) 264.
13. R.C. Cammarata, C.V. Thompson, and S.M. Garrison, Proc. Mat. Res. Soc. 92 (1987) 335.

## FIGURE CAPTIONS

1. RHEED micrographs of a SiGe film a) oxidized at 900°C for 30 minutes, b) annealed in vacuum at 850°C for 60 minutes, c,d) oxidized at 900°C for 60 minutes, and e,f) oxidized at 900°C for 120 minutes.

2. Random and channeling Rutherford Backscattering Spectra using a $3Me^{4}He^{++}$ beam at an angle of 170°. The sample is a SiGe thin film oxidized at 900°C for 120 minutes.

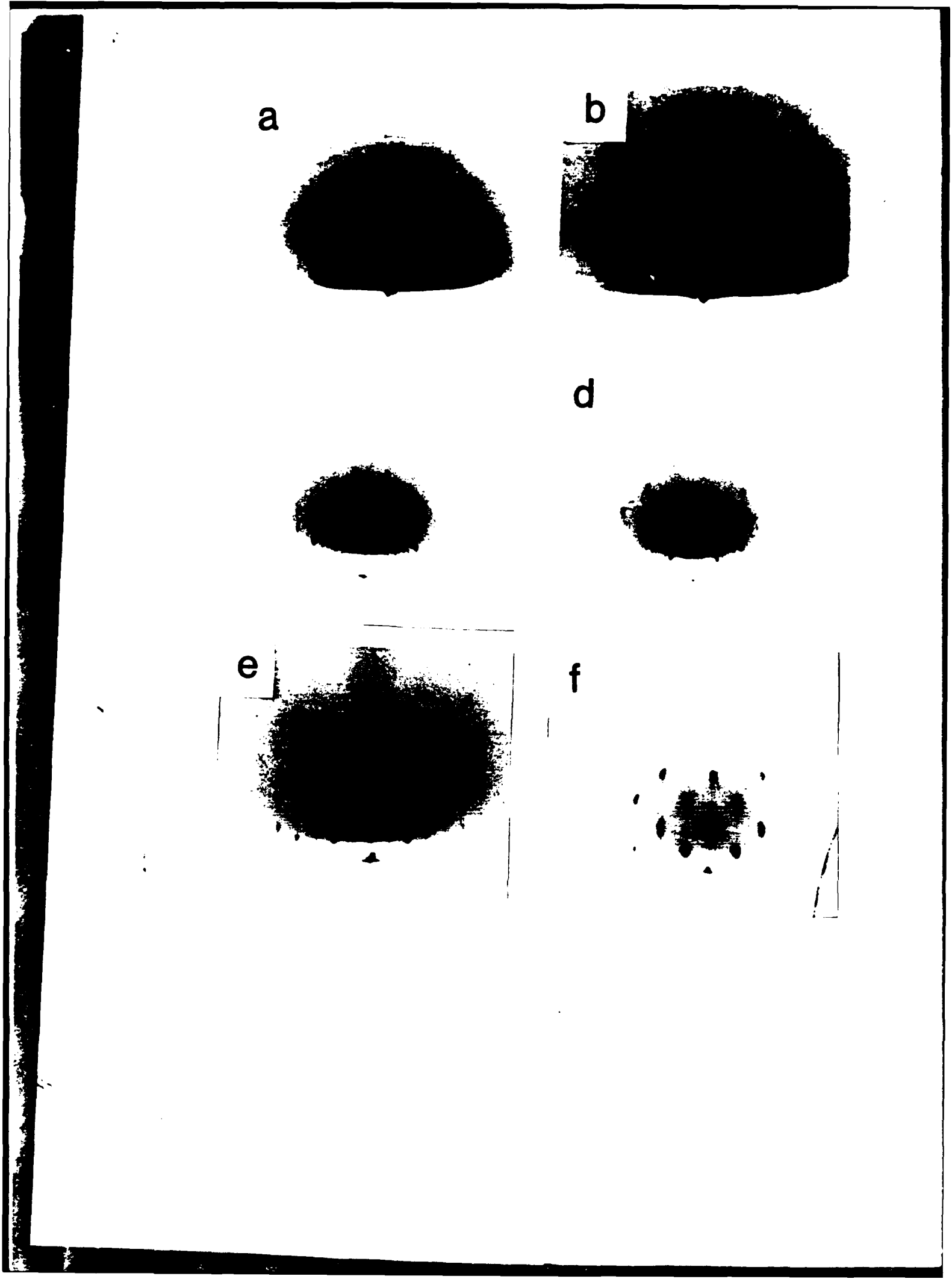
a
b
d
e
f

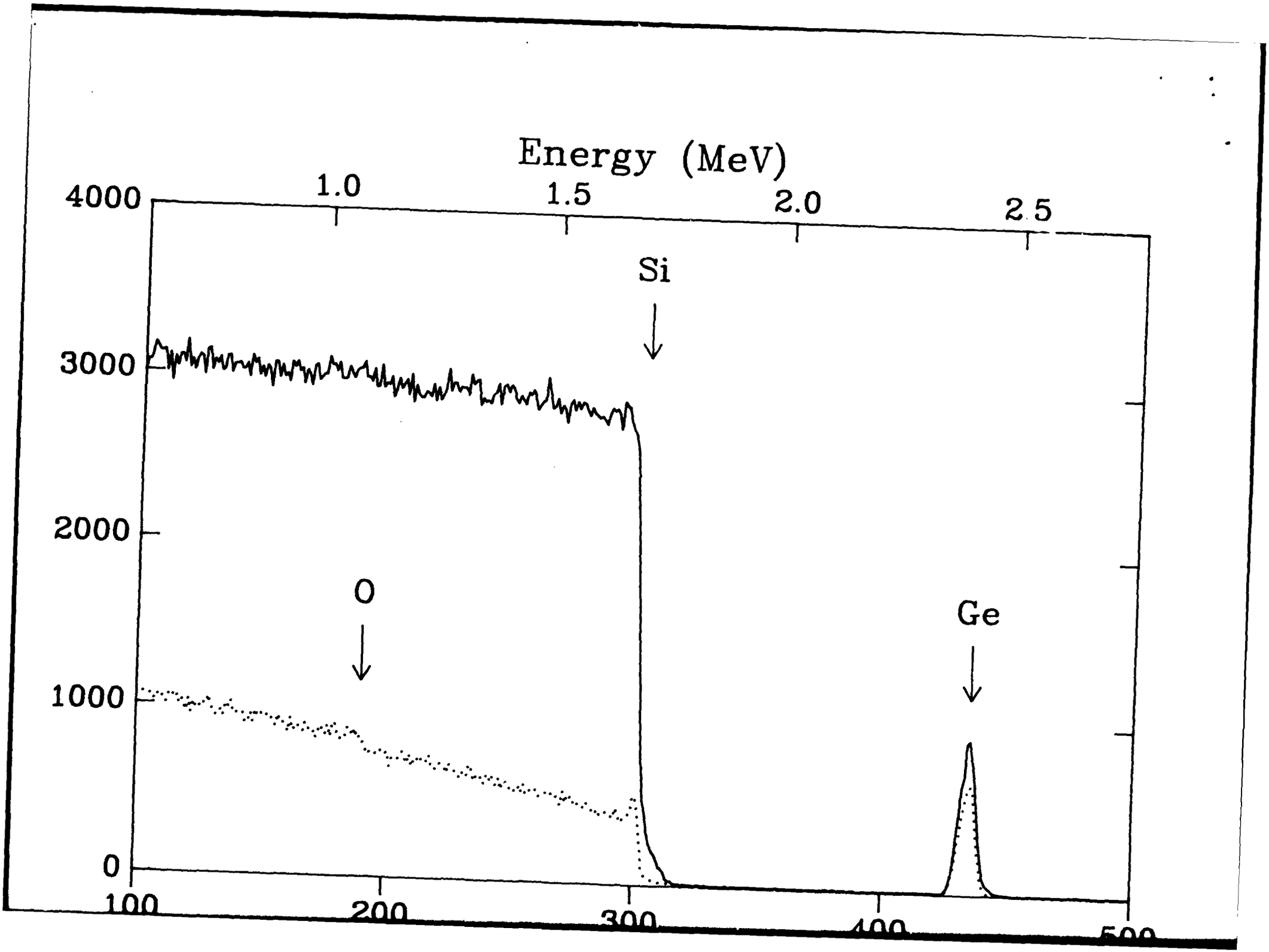
Energy (MeV)
1.0
1.5
2.0
2.5
4000
3000
2000
1000
0
Si
O
Ge
100
200
300
400
500

# ETCH PIT PATTERNS OF MISFIT DISLOCATIONS IN AlGaAs/GaAs HETEROSTRUCTURES

W. TSENG, S. PROKES, B. WILKINS, M. FATEMI and A. CHRISTOU
*Naval Research Laboratory, Washington, D.C. 20375, USA*

Received 15 December 1987; in final form 1 March 1988

Misfit dislocations at the $Al_{0.3}Ga_{0.7}As/GaAs$ heterojunction have been revealed by an etching technique on the cleaved interface. On the $(1\bar{1}0)$ cleaved surfaces, the dislocation etch pits are revealed as upright pyramids, while on the (110) surfaces, i.e. parallel to the primary flat, they are revealed as inverted pyramids.

A heterostructure creating elastic *strain* may or may not be commensurate depending upon the amount of lattice mismatch and layer thickness [1]. Generally, when the lattice mismatch and/or the layer thickness is large, the strained heterostructure will not be commensurate. The strain will be relieved by the formation of misfit dislocations and by an increase of the dislocation density in the vicinity of the interface. In this Letter, we describe a simple technique using warm HF as an etchant to reveal misfit dislocations in the AlGaAs/GaAs heterostructure.

The substrates were commercially polished, (001) oriented, semi-insulating GaAs wafers. The GaAs and AlGaAs were deposited by molecular beam epitaxy in a VG Semicon V8OH MBE system. After the removal of 3 to 5 μm of GaAs in a 7:1:1 sulfuric acid:water:hydrogen peroxide solution, the substrates had a thin, desorbable oxide. After the oxide layer was removed, RHEED showed a $2\times(4)$ As-stabilized reconstruction pattern when the electron beam was perpendicular to the secondary flat of these GaAs wafers (i.e. the e-beam was along the $(1\bar{1}0)$ azimuth), whereas a $4\times(2)$ pattern was observed when the e-beam was perpendicular to the primary flat (i.e. (110) azimuth). Successive MBE layers were then grown, forming the following structure:

GaAs substrate | GaAs buffer (1 μm) |

| AlGaAs (1.8 μm) | GaAs cap (0.3 μm) .

The experimental conditions for the Ga and As fluxes were established in order to give a growth rate of 0.9 μm/h.

The Al fraction in the AlGaAs layers was determined by X-ray rocking curves. The AlGaAs peak appeared 95 arcseconds below the GaAs peak as shown in fig. 1. From this, the Al fraction was calculated to be 29.2%, based on a 325 arcsecond shift

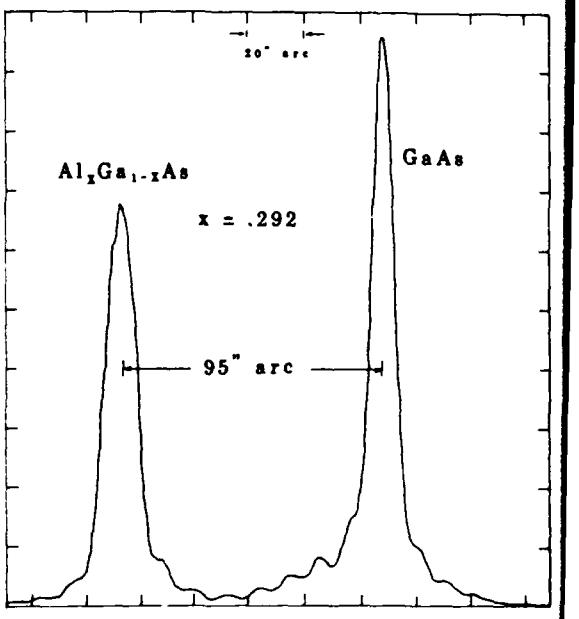


Fig. 1. X-ray rocking curve of a AlGaAs/GaAs heterostructure.

0167-577x/88/$ 03.50 

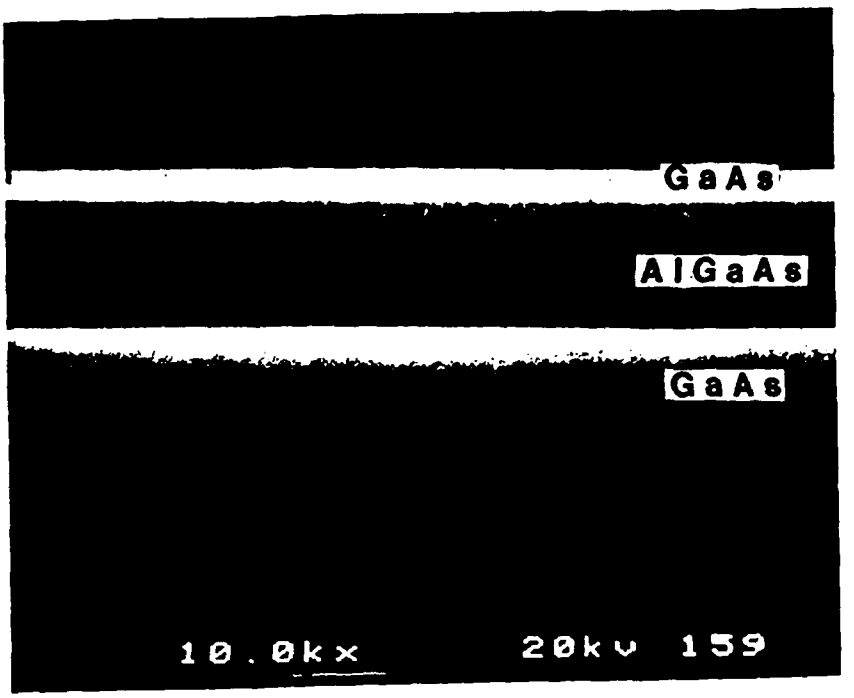


Fig. 2. SEM micrograph of a cross-sectional AlGaAs/GaAs sample etched in concentrated HF at 90°C for 4 min. The etched groove (i.e. the AlGaAs layer) is 1.8 μm wide.

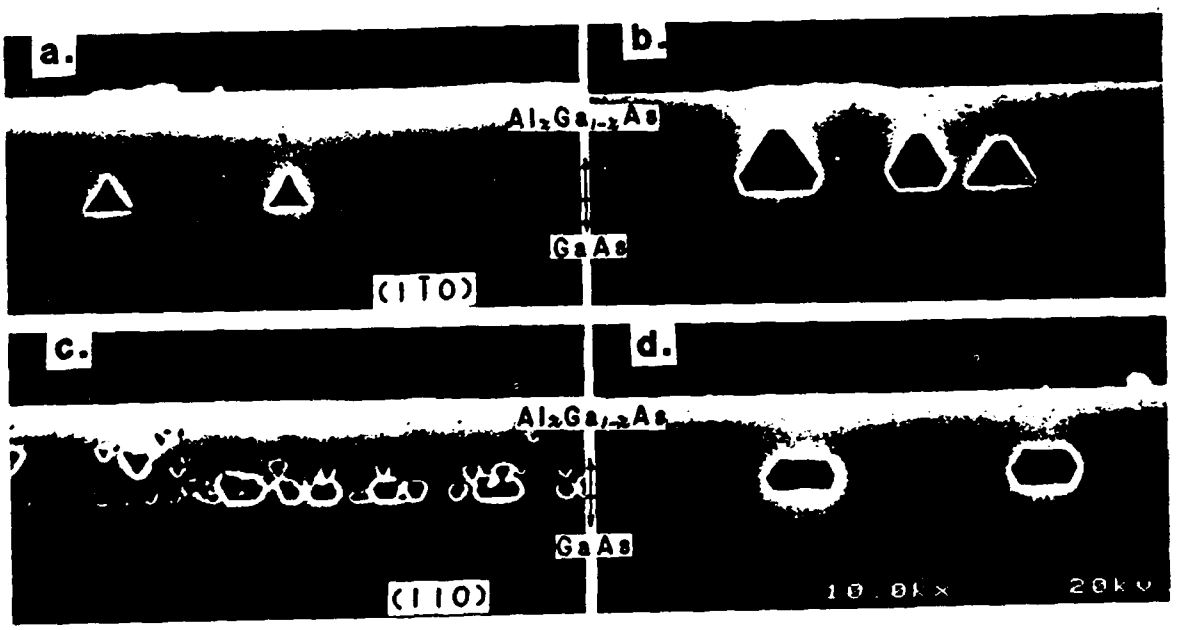


Fig. 3. SEM cross-sectional views of AlGaAs/GaAs samples etched in concentrated HF at 70°C on (1$\bar{1}$0) planes for (a) 2 min and (b) 4 min, and on (110) planes for (c) 2 min and (d) 4 min.

from GaAs for AlAs with 100% Al[#1]. This figure clearly shows a lattice mismatch between AlGaAs and GaAs, of the order of 0.037%.

In order to reveal the crystallographic defects by etching, the samples were cleaved parallel to either a primary or secondary flat of the wafer. The etchant is a standard concentrated 49% HF solution (made by Fisher scientific). A warm water bath with a thermometer was heated to a desired temperature between 50 and 95°C, and a Nalgene beaker containing concentrated HF was placed in the warm bath for 3 min in order to stabilize the solution temperature. The cleaved samples were then dropped in the warm HF solution for 2 to 5 min, removed, rinsed in deionized water and blown dry.

The AlGaAs layer was removed uniformly at etch temperatures higher than 80°C, as shown in fig. 2. At temperature lower than 80°C, the defected regions in the AlGaAs were etched preferentially. Fig. 3 shows the etch pit patterns on $(1\bar{1}0)$ and (110) cleaved planes. On the $(1\bar{1}0)$ plane, the patterns appear as regular pyramids as shown in fig. 3a, while on the (110) plane, the patterns are inverted pyramids shown in fig. 3c. The sidewalls of the etch patterns are {111} planes. If the samples were etched longer, the etched patterns became six-sided polygons, shown in figs. 3b and 3d.

The defect associated with the etch pattern was identified by cross-sectional transmission electron microscopy (XTEM). The defect observed is an edge type dislocation, located near the AlGaAs/GaAs interface, as shown in fig. 4. From the separation distances (1 to 5 μm) between the dislocations observed in the TEM and the separation distances (also 1 to 5 μm) between etch pits, one may conclude that the etch pits are due to misfit dislocations.

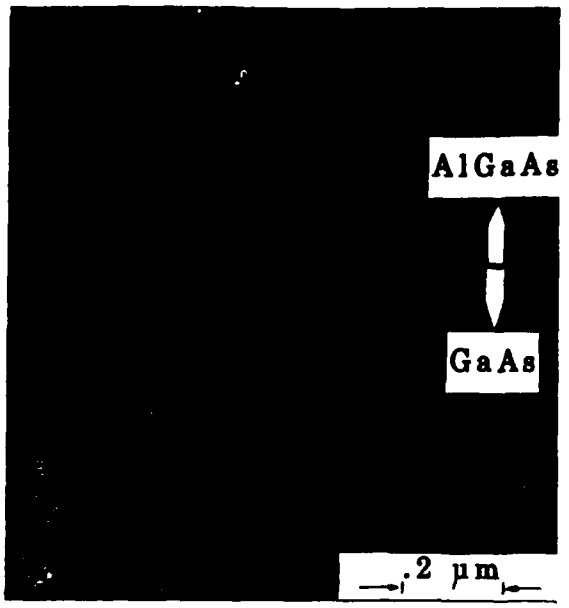


Fig. 4. Cross-sectional TEM micrograph of AlGaAs/GaAs heterostructure, showing a misfit dislocation. The magnification marker was calibrated to the 1.8 μm AlGaAs layer observed from the difference in image contrast with the GaAs.

In summary, a simple warm HF solution can be used to reveal misfit dislocations in AlGaAs/GaAs heterostructures, thereby eliminating the use of more labor-intensive characterization techniques such as XTEM.

[#1] The Al fraction was also routinely determined by photoluminescence and photoreflectance measurements. The X-ray results are generally 2% higher than the results from the above two methods in the range of 20 to 40% Al fractions.

## Reference

[1] R. Hull, J.C. Bean, F. Cerdeira, A.T. Fiory and J.M. Gibson, Appl. Phys. Letters 48 (1986) 56.

To be published in MRS Proceedings, Dec 1988

# THE MECHANISM OF EPITAXIAL $Si_{1-x}Ge_x$ FILM FORMATION PRODUCED BY THE OXIDATION OF AMORPHOUS SiGe LAYERS DEPOSITED ON Si(100).

S.M. PROKES*, W.F. TSENG, AND A. CHRISTOU
Naval Research Laboratory, Code 6832, Washigton, D.C. 20375.
* ONT Postdoctoral Fellow

## INTRODUCTION

In general, high quality epitaxial SiGe heterostructures can be produced by such techniques as molecular beam epitaxy (MBE)[1] or chemical vapor deposition (CVD)[2]. These techniques, especially MBE, allow precise monolayer control, thus allowing the tailoring of the transport and optical properties of this system [3]. However, these growth techniques require extremely low interfacial contamination of the substrate, and precise temperature control.

The formation of epitaxial Si and Ge heterostructures has also been investigated by solid-phase epitaxial regrowth (SPE) of evaporated amorphous films [4,5,6]. Results indicate that a very clean interface between the Si substrate and the amorphous layer must exist before SPE can occur.

Recently, pulsed laser annealing has also been used to achieve SPE of amorphous Ge layers on Si(100) [7]. In this case, the Si and amorphous Ge interface was melted during laser annealing, allowing SPE to occur. An additional epitaxial regrowth technique has been reported by Fathy et al. [8], in which Ge implanted Si(100) samples were oxidized under a steam ambient, creating an epitaxial SiGe layer directly beneath the $SiO_2$.

In this work, we have formed an epitaxial, SiGe/Si heterostructure from an initially amorphous Ge and SiGe alloy evaporated on Si(100). Wet oxidation has been used, and it has been found that interfacial contamination is not critical in the epitaxial layer formation, due to the kinetics associated with the rapid oxidation process.

## SAMPLE PREPARATION

The substrates used were Si(100) wafers, boron-doped to 300 ohm-cm. The substrates were RCA cleaned, and loaded into a standard electron-beam evaporator, at a background pressure of $1x10^{-7}$ torr. Amorphous Ge, $Si_{0.86}Ge_{0.14}$, $Si_{0.70}Ge_{0.30}$, and $Si_{0.56}Ge_{0.44}$ layers 1000Å thick were deposited at a rate of 2Å/s directly onto the RCA cleaned Si(100) held at room temperature. Following deposition, the samples were cut into 2cm x 2cm pieces, and rinsed in trichloroethylene, acetone, and methanol, followed by a dip in HF for 10 seconds. The samples were loaded into an open tube furnace, flushed with nitrogen, and brought to 900°C in a steam ambient for various time periods.

## SAMPLE CHARACTERIZATION

After stripping the oxide in HF, the samples were first characterized using reflected electron diffraction (RED), with results shown in Fig. 1 for a sample of $Si_{0.86}Ge_{0.14}$, oxidized or annealed for various times. The sample was oxidized as follows: 1a) 30 minutes, 1c,d) 60 minutes, and 1e,f) 120 minutes, all at 900°C. It is clear that the sample undergoes a transition from polycrystalline (in 1a) to part poly, part single crystal (in 1c,d) to fully single crystal (in 1e,f).

Two additional samples were annealed, one in UHV ($8x10^{-10}$ torr) and the other at ambient pressure, in an nitrogen atmosphere. The RED micrograph of the sample, which was annealed at 850°C for 60 minutes, is shown in Fig. 1b. The sample appears to be fully polycrystalline. The second sample, annealed for 120 minutes at 900°C in nitrogen, also exhibited a fully polycrystalline structure when examined by X-ray diffraction. This result indicates that the initial Si/amorphous SiGe interface contains a relatively thick native oxide layer, in which SPE cannot occur under normal annealing conditions.

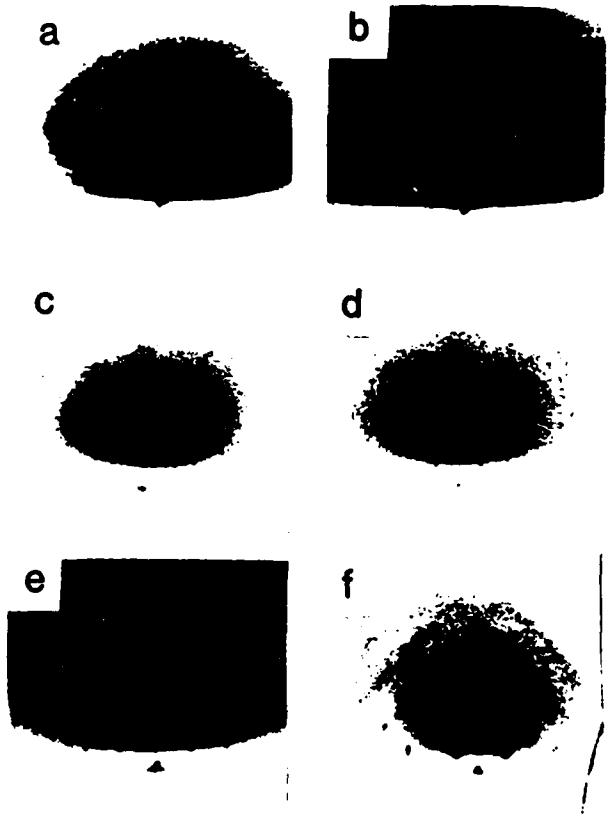


Fig 1. RED micrographs of a $Si_{0.86}Ge_{0.14}$ film a) oxidized at 900°C for 30 minutes, b) annealed in vacuum at 850°C for 60 minutes, c,d) oxidized at 900°C for 60 minutes, and e,f) oxidized at 900°C for 120 minutes.

Rutherford backscattering has also been used in order to determine the crystallinity and thickness of these epitaxial heterostructures. Results indicate that samples exhibiting the single phase pattern of Fig. 1e,f were single crystal, and a 500Å, germanium-rich layer was present in the $Si_{0.86}Ge_{0.14}$ sample oxidized at 900°C for 120 minutes.

The germanium concentration in the epitaxial layer has also been measured using Raman Spectroscopy, showing a higher germanium concentration in the epitaxial layer than in the initial amorphous SiGe films. This Raman technique is described elsewhere [9].

Transmission electron microscopy has also been used in order to determine the microstructures present in the samples shown in Fig. 1. Results indicate the presence of single crystal regions for the samples described in Fig. 1c,d, and the samples of Fig. 1e,f appear fully single crystal. Moire fringes were also apparent in these images, due to the Si and Ge lattice variation.

## DISCUSSION

A mechanism to explain the above results is suggested, involving the diffusion of silicon through the native oxide, which allows the SiGe alloy to orient with respect to the underlying Si(100) substrate. The epitaxial SiGe layer formation is also discussed in terms of solid phase epitaxial regrowth versus secondary grain growth.

## REFERENCES


1. J.C. Bean, L.C. Feldman, A.T. Fiory, S. Nakahara, and I.K. Robinson, J. Vac. Sci. Technol. A2 (1984) 436.

2. C.M. Gronet, C.A. King, W. Opyd, J.F. Gibbons, S.D. Wilson, and R. Hull, J. Appl. Phys. 61 (1987) 2407.

3. J. Bevk,J.P. Mannaerts, L.C. Feldmanm, B.A. Davidson, and A. Ourmazd, Appl. Phys. Lett. 49 (1986) 286.

4. M. von Allmen, S.S. Lau, D.M. Scott, J.W. Mayer, W.F. Tseng, T.T. Sheng, P. Williams, and J.E. Baker, Proceedings of Symposium on Thin Film Interfaces and Interactions, Electrochemical Soc. 80(2) (1980) 195.

5. M.G. Grimaldi, M. Maenpaa, B.M. Paine, M-A. Nicolet, S.S. Lau, and W.F. Tseng, J. Appl. Phys. 52 (1981) 1351.

6. L.S. Hung, S.S. Lau, M. von Allmen, J.W. Mayer, B.M. Ulrich, J.E. Baker, P. Williams, and W.F. Tseng, Appl. Phys. Lett. 37 (1980) 909.

7. J.R. Abelson, T.W. Sigmon, Ki Bum Kim, and K.H. Weiner, Appl. Phys. Lett. 52 (1988) 230.

8. D. Fathy, O.W. Holland, and C.W. White, Appl. Phys. Lett. 51 (1987) 1337.

9. S.M. Prokes, O.J. Glembocki, E.P. Donovan, R. Stahlbush, W.E. Carlos, H. Dietrich and A. Christou, Proceedings on Spectroscopic Characterization Techniques for Semiconductor Technology III, SPIE 946 (1988) 204.

Published in Proceedings of the SPIE
Vol 946, (1988) 204

# Study of thin epitaxial film formation by germanium segregation in silicon oxidation

S.M. Prokes,* O.J. Glembocki, E.P. Donovan, R. Stahlbush,
W.E. Carlos, H. Dietrich, and A. Christou

Naval Research Laboratory
Washington, D.C. 20375

## ABSTRACT

Thin germanium-rich layers have been formed by the implantation of Ge into Si substrates, followed by a wet oxidation process. We have measured the germanium concentration profile of layers formed by this method for samples initially implanted to a dose of $1 \times 10^{17}cm^{-2}$. Structural, optical, and electronic probes have been used, all of which yield similar results. The results from Rutherford backscattering (RBS), Auger spectroscopy (AES), Raman spectroscopy, and electroreflectance (ER) show that the germanium-rich layer is about 300Å thick, and contains an average germanium concentration of 65%. The SiGe/Si interface is not sharp but diffuse, with a decreasing germanium concentration. In addition, the data suggest a thin layer of $Si_{13}Ge_{87}$ near the $SiO_2$/SiGe interface.

## 1. INTRODUCTION

It has recently been reported that epitaxial $Si_{1-x}Ge_x$ films can be formed by germanium implantation followed by a steam oxidation.[1] During the oxidation process, the germanium segregates at the $Si/SiO_2$ interface, forming a thin epitaxial germanium-rich layer sandwiched between the Si substrate and an $SiO_2$ film. These layers are strained and commensurate with the Si substrate for low implantation doses, but become incommensurate for higher doses ($1 \times 10^{17}/cm^2$ at 150keV).

An enhanced oxidation rate has been measured for these samples, with no measurable germanium incorporation into the oxide.[2] This enhanced oxide formation result may be due to a change in interface oxidation kinetics,[3] assuming that the diffusion of silicon into the germanium is not a rate limiting step. This model is consistent with previous reports of rapid diffusion of silicon into germanium for Si/Ge superlattices.[4]

In this paper, the germanium concentration of these films is examined. Some evidence suggests the existence of two layers of different Ge concentration within the $Si_{1-x}Ge_x$ epitaxial films. These results have been obtained by the use of electroreflectance, Raman spectroscopy, Rutherford backscattering, and Auger electron spectroscopy.

## 2. EXPERIMENTAL PROCEDURES

Single *p*-type Si(100) crystals with resistivities between 25 and 45 ohm-cm were implanted at room temperature, using singly charged 150 keV $^{74}Ge^+$ ions. Prior to oxidation, the samples were

*ONT Postdoctoral Fellow

dipped in HF, followed by a rinse in hot trichloroethylene, acetone, and methanol. The samples were then introduced into a tube furnace and nitrogen was flushed through for ten minutes. The furnace was brought to a temperature of 900°C, at which time oxygen bubbled through a boiling water bath was passed over the sample. The oxidation temperature was monitored using a thermocouple attached directly to the sample holder. A silicon control sample was included in each run to properly monitor the oxide thickness. Samples implanted with $1 \times 10^{16}$, $3 \times 10^{16}$, and $1 \times 10^{17}$ Ge/cm$^2$ were oxidized for 100 minutes, at 900°C.

## 3. RESULTS

*Rutherford backscattering* (RBS) was used to measure surface concentration profiles using 2 MeV $He^+$ ions at a scattering angle of 45°. Figure 1 shows the random backscattering yield for a sample implanted to $1 \times 10^{17}$/cm$^2$ and oxidized at 900°C for 100 minutes. A germanium peak is clearly visible at about 1.52 MeV, which corresponds to a buried germanium layer. The solid line refers to a simulation of the backscattering yield, which has been obtained using the Cornell University RUMP program.[5] From this data, it is clear that there is a germanium-rich layer beneath the oxide, which is 2400Å thick. Figure 2 shows the data and several simulations of the germanium peak. The simulations show the results expected for (1) a 240Å, 80% Ge buried layer, (2) a 311Å, 60% Ge layer and (3) a 250Å, 60% Ge layer followed by two transitional layers of decreasing Ge

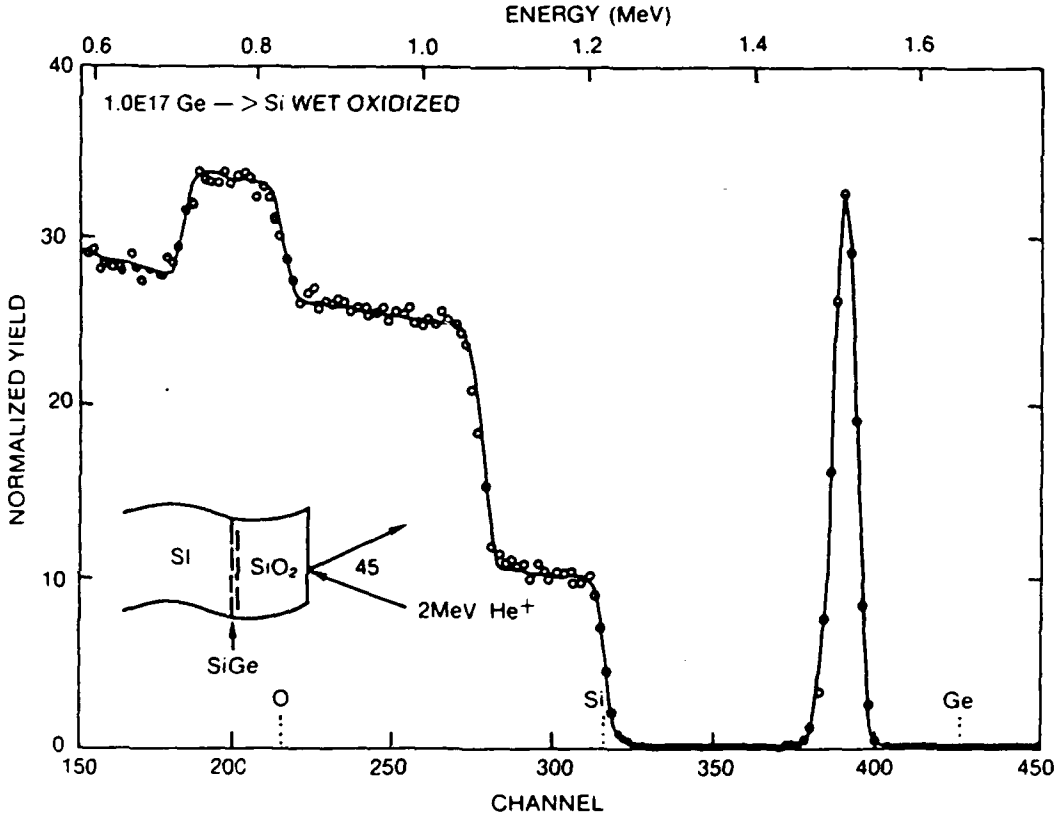


Figure 1. Rutherford backscattering spectrum (open circles) of $1 \times 10^{17}$ Ge/cm$^2$ implanted sample and oxidized for 100 minutes at 900°C. Solid line shows the fit to the data using the Cornell RUMP simulation program.[5]

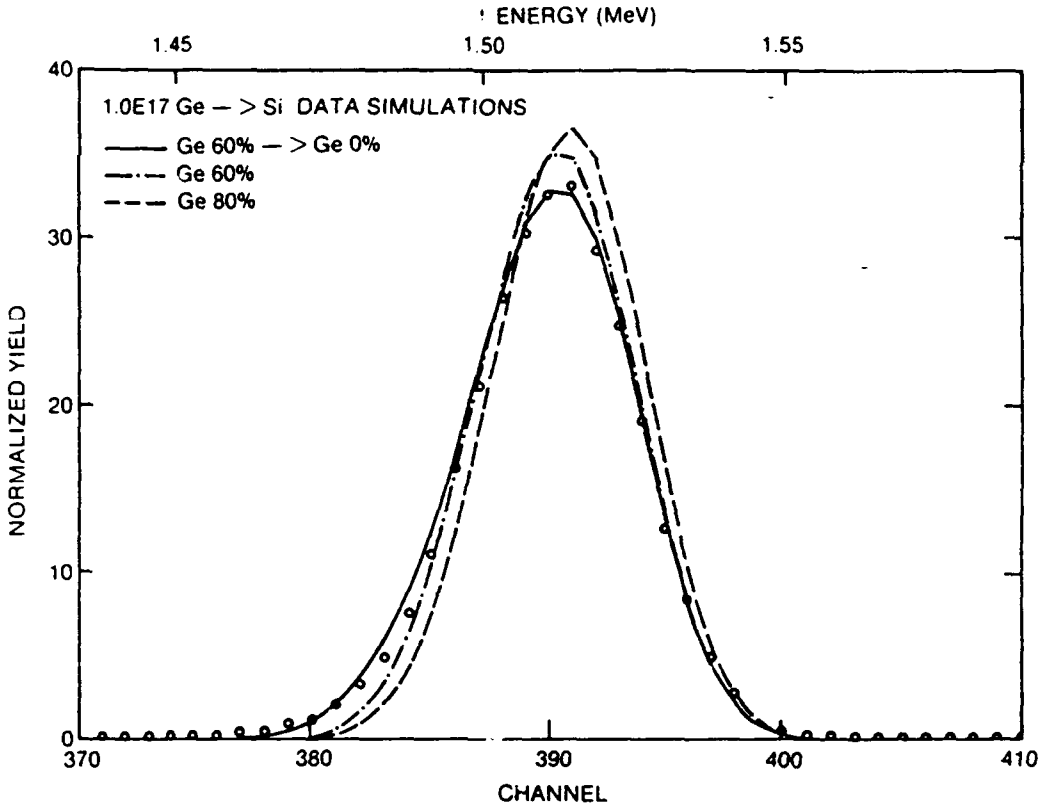


Figure 2. Rutherford backscattering spectrum of Fig. 1, limited to the energy of the Ge peak (open circles) and three RUMP simulations. The simulations are as follows: 1. (Ge 80%) 247Å layer of $Si_{.2}Ge_{.8}$, 2. (Ge 60%) 311Å layer of $Si_{.4}Ge_{.6}$, and 3. (Ge 60%->Ge 0%) 250Å layer of $Si_{.4}Ge_{.6}$, 100Å layer of $Si_{.8}Ge_{.2}$, and 200Å layer of $Si_{.91}Ge_{.09}$. All parameters were chosen to give a total Ge concentration of $1 \times 10^{17}/cm^2$.

concentration (all simulations refer to the same integrated Ge concentration). Clearly, the introduction of a gradual decrease in the Ge concentration between the Ge-rich layer and the underlying substrate yields a better fit. Thus, it appears that the average Ge concentration in this layer is not as high as has been reported[1,3] in similar studies.

Further evidence of the concentration profile of the $Si_{1-x}Ge_x$ layer can be seen by Auger electron spectroscopy, shown in Figure 3. The germanium peak appears at the oxide interface and consists of roughly 55% germanium. The layer thickness is about 270Å, but the peak shows a definite asymmetry at the $Si_{1-x}Ge_x$/Si interface, suggesting that this interface is diffuse, in agreement with the RBS data.

Both vibrational spectroscopy using Raman scattering and interband spectroscopy using electroreflectance were used to characterize the amount of alloying in this thin $Si_{1-x}Ge_x$ layer. In Raman scattering, we can probe the modes associated with Si-Si, Si-Ge, and Ge-Ge vibrations of the alloy lattice and from the peak positions of the Raman lines we can determine the concentration of the Ge in the alloy, $x$. Feldman et al.[6] suggest that the frequency of the Si-Ge vibration should follow:

$$\nu = A + B(1 - x) \tag{1}$$

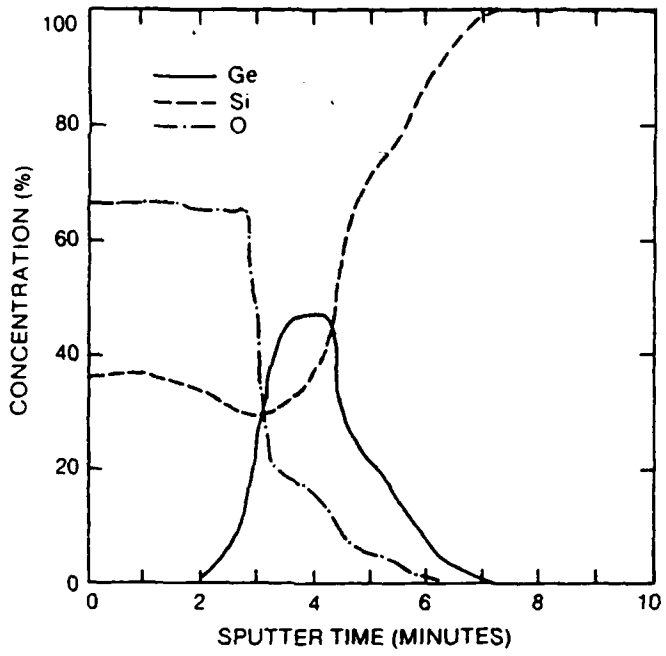


Figure 3. Auger spectrum of a sample implanted to 1 $\times$ $10^{17}$ Ge/cm$^2$, oxidized for 100 min. at 900°C. Sputtering voltage was 2000V and the sputter rate was 100Å/min.

The values of $A$ can vary from a theoretical value of 392 cm$^{-1}$ to Feldman's value of 389 $\pm$ 2.0 cm$^{-1}$, while $B$ is given by 050 $\pm$ 010. Shown in Fig. (4) is the Raman spectrum for the sample with the highest implant fluence (1 $\times$ $10^{17}$/cm$^2$) at the 5145Å line of an $Ar^+$ ion laser, operating at 200 mV. The diameter of the laser spot was 100$\mu$m. At this wavelength, the light penetrates through the thin alloy and deep into the Si substrate. Four peaks are readily visible. The largest intensity peak is from the Si substrate and occurs at 521 cm$^{-1}$. The next lowest frequency line is at 470.1 cm$^{-1}$ and is associated with Si-pair vibrations in the alloy. The strong feature at 296.4 cm$^{-1}$ is from Ge-Ge local modes, while the feature at 406.5 cm$^{-1}$ is due to Si-Ge vibrations. The alloy lines, Ge-Ge and Si-Ge are asymmetrically broadened toward lower frequencies. While other authors have suggested that this broadening in strained layers is due to both dislocations and strain,[7] our sample is not expected to be strained due to the thickness and large $x$ value ($x \approx .6$ from RBS).[8] We feel that for this sample, the asymmetry is due to alloy disorder. Using Eq. 1 for the frequency of the Si-Ge line, along with Feldman's values for $A$ and $B$ we find that $x \approx 0.65$, in good agreement with RBS and Auger. Similarly, we can find $x$ values of .404 and .36 for samples implanted to 3 $\times$ $10^{16}$ and 1 $\times$ $10^{16}$, respectively. There is clearly a trend to lower Ge concentration for lower implantation doses. However, there is about 15% uncertainty in the $x$ value due to the uncertainty in $B$.

In order to obtain a better value for $x$ optically and to explore the band structure properties of the alloy layer, we utilized electroreflectance (ER). This technique measures interband transitions of the alloy for the first two direct gaps, $E_0$ and $E_1$. Kline et al.[9] measured the ER spectra for bulk $Si_{1-x}Ge_x$ alloys over the entire concentration range. A very important result is that the $E_0$ transitions vary by nearly 3eV as the concentration varies from pure Ge to pure Si, and the $E_1$ transition changes by 1eV. With such a large variation in gaps, it is possible to obtain a good value for $x$.

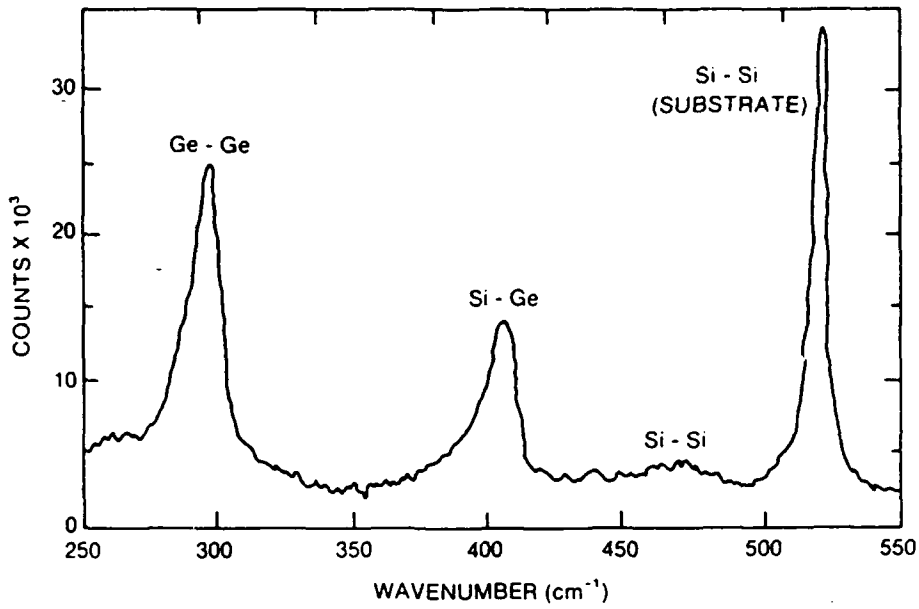


Figure 4. Raman spectrum of sample from Fig. 1, showing three Raman lines from the alloy layer and one from the Si substrate.

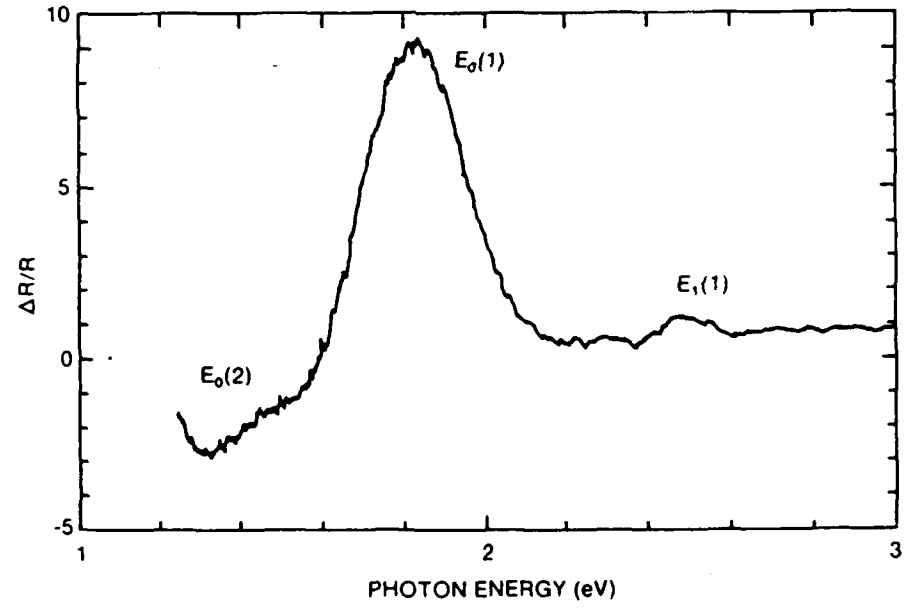


Figure 5. Electroreflectance data of sample from Fig.1. The first two direct band transitions, $E_0(1)$ and $E_1(1)$, are shown for the 60% layer, as well as the $E_0(2)$ direct band transition of an 87% Ge layer.

The ER measurements were performed using a standard spectrometer widely described in the literature (F.H. Pollak and O.J. Glembocki, this conference and references therein).[10] The field was applied in an MOS configuration using a 100 Å transparent Cr gate and 2500 Å of $SiO_2$. A square wave of 15V peak to peak at 500 Hz was used to form the modulating field. Shown in Fig. 5 is the ER spectrum of the sample with the highest dose ($1 \times 10^{17}$ cm$^{-2}$) over the range of 1 to 3 eV. The peaks were taken as the transition energies, which are consistent with Kline et al.[9] The largest peak, labeled $E_0(1)$ is due to $E_0$ transitions from the $Si_{1-x}Ge_x$ alloy. This gives an $x$ value of .67, in very good agreement with our other results. The low intensity peak at higher energies, labeled $E_1(1)$, is the corresponding $E_1$ transition, giving an $x$ value of .70. The value of $x$ deduced from the $E_0$ transition is greater than from the $E_1$ transition, a range over which the penetration depth of light decreases from about 1$\mu$m at $E_0$ to under 500 Å at $E_1$. This change may be due to an increasing Ge content with decreasing depth of the alloy layer. The RBS data support such a model. The ER data also show that there is a second, higher concentration layer. The structure near 1.37 eV labeled $E_0(2)$, is assigned to the $E_0$ transition of this layer and gives an $x$ value of .87. It is assumed that this thin layer is near the $SiO_2/Si_{1-x}Ge_x$ interface. Due to instrumental difficulties, we were unable to perform measurements below 1.3 eV and could not obtain the full line shape of this feature.

From the large line width, $\Gamma_1$, of the $E_0(1)$ line the $x$ variations in this sample can be estimated. Assuming that the main contribution to $\Gamma$ is due to spacial variations in $x$, we find that $\delta x \approx 0.10$, which is in accord with RBS data. The line width of the $E_1(1)$ transition gives a value of $\delta x \approx 0.12$.

## 4. CONCLUSIONS

In conclusion, we have measured the germanium concentration profile of layers formed by oxidizing $1 \times 10^{17}$ cm$^{-2}$ Ge implant. Rutherford backscattering, Auger electron spectroscopy, Raman scattering, and electroreflectance have been used, and all lead to similar results. The germanium-rich layer is about 300 Å thick and most of the layer has a Ge concentration between 60% and 70%. In addition, the data suggest that there is a thin layer of higher Ge concentration near the $SiO_2$/SiGe interface. Finally, the SiGe/Si interface is not sharp, but diffuse, having a gradual decrease of the Ge concentration.

## 5. REFERENCES


1. D. Fathy, O.W. Holland, and C.W. White, Appl. Phys. Lett. **51** (1987) 1337.

2. O.W. Holland, C.W. White, and D. Fathy, Appl. Phys. Lett. **51** (1987) 520.

3. E.C. Frey, N.R. Parikh, M.L. Swanson, M.Z. Numan, and W.K. Chu, Proceedings of the Materials Research Society, to be published.

4. S.M. Prokes and F. Spaepen, Appl. Phys. Lett. **47** (1985) 234.

5. The authors have used the program RUMP from Cornell University (see L.R. Doolittle, Nucl. Instr. and Meth. **B9**(1983) 344) to analyze the RBS spectra.

6. D.W. Feldman, M. Ashkin, and James H. Parker, Jr., Phys. Rev. Lett. **17** (1966) 1209.

7. F. Cerdeira, A. Pinczuk, J.C. Bean, B. Batlogg, and B.A. Wilson, Appl. Phys. Lett. **45** (1984) 1138.

8. T.P. Pearsall, F.H. Pollak, J.C. Bean, and R. Hull, Phys. Rev. **B33** (1986) 33.

9. J.S. Kline, F.H. Pollak, and M. Cardona, Helvetica Physica Acta **41** (1968) 968.

10. F.H. Pollack and O.J. Glembocki, this conference and references therein.

To be published in MRS proceedings VIIV, 1988.

# MBE GROWTH AND CHARACTERIZATION OF GaAs THIN FILMS ON SiGe BUFFER LAYERS

S.M. PROKES*, W.F. TSENG,** B.R. WILKINS,** H. DIETRICH,** AND A. CHRISTOU**
*ONT/NRL Post-Doctoral Fellow
**Naval Research Laboratory, Washington, DC 20375-5000

## ABSTRACT

Epitaxial SiGe buffers have been formed by the implantation of $^{74}Ge^{+}$ ions into Si(100)4° to <011> substrates. The implants were made at 150keV to a dose of $1x10^{17}/cm^2$. The epitaxial layers were characterized by Rutherford backscattering, Raman spectroscopy, and electroreflectance and were found to be 300Å thick having on average a composition of $Si_{0.35}Ge_{0.65}$. GaAs layers were then grown on these substrates by molecular beam epitaxy, using the standard two-step growth process. The results from Auger, Scanning Electron Microscopy, and Cross-sectional TEM indicate a lower defect production and propagation in these samples, compared to those grown directly on Si.

## INTRODUCTION

In recent years, epitaxial growth of GaAs on Si has drawn increasing interest since such a system presents possibilities for novel integrated device structures. Although success has been reported in the suppression of antiphase domains [1-3], a major problem still remains. The 4% lattice mismatch and the large difference in the thermal expansion coefficients of GaAs and Si lead to a relatively high dislocation density which is much greater than that of bulk GaAs [4].

There are several approaches which can be utilized to reduce the threading dislocation density. One is the use of a strained superlattice buffer layer such as InGaAs/GaAs which minimizes the threading of dislocations from the interface. Misoriented Si substrates can also help suppress dislocation propagation [4,5]. Ideally, the best solution is to reduce the number of misfit dislocations created at the interface by using a properly chosen buffer layer. Since germanium has only a .35% lattice mismatch to GaAs, and has a very similar thermal expansion coefficient, it is an ideal candidate for this buffer layer. Previous work has involved GaAs growth on Ge substrates [6,7] or GaAs growth on Ge layers on Si which necessitated two separate UHV growth processes [8]. In this work, we have prepared epitaxial SiGe buffer layers by a novel technique consisting of implantation and oxidation of Si wafers [9] which were then used as substrates for the MBE growth of GaAs. Thus, only a GaAs MBE was necessary to grow GaAs/SiGe/Si heterostructures.

## SUBSTRATE PREPARATION

It has recently been reported that epitaxial $Si_{1-x}Ge_x$ films can be formed by germanium implantation followed by a steam oxidation [9]. During the oxidation process the germanium segregates at the $Si/SiO_2$ interface forming a thin, epitaxial, germanium-rich layer just beneath the oxide. This procedure was utilized to produce the required SiGe buffer layers for the GaAs growth.

Single, p-type Si(100) 4° to <011> wafers with resistivities between 25 and 45 ohm-cm were implanted at room temperature using singly charged 150KeV $^{74}Ge^{+}$ ions. The implantation dose was $1x10^{17}$ Ge/cm$^2$. Prior to oxidation the samples were rinsed in hot trichloroethylene, acetone, and methanol followed

by a dip in HF. They were then introduced into a tube furnace and oxidized at 900°C for 100 minutes.

The resulting layers were then analyzed by the use of Rutherford backscattering, Raman spectroscopy, electro-reflectance, and reflective high energy electron diffraction (RHEED) [10].

Rutherford backscattering (RBS) was used to measure surface concentration profiles using 2MeV He+ ions at a scattering angle of 45°. Figure 1 shows the random back-scattering yield for the sample. The solid line is a simulation of the backscattering yield which has been obtained using the Cornell University RUMP program [11]. The germanium-rich layer is directly beneath the 2400Å oxide layer as the simulation suggests, and it contains 250Å of $Si_{0.4}Ge_{0.6}$ followed by a transitional layer of decreasing Ge concentration.

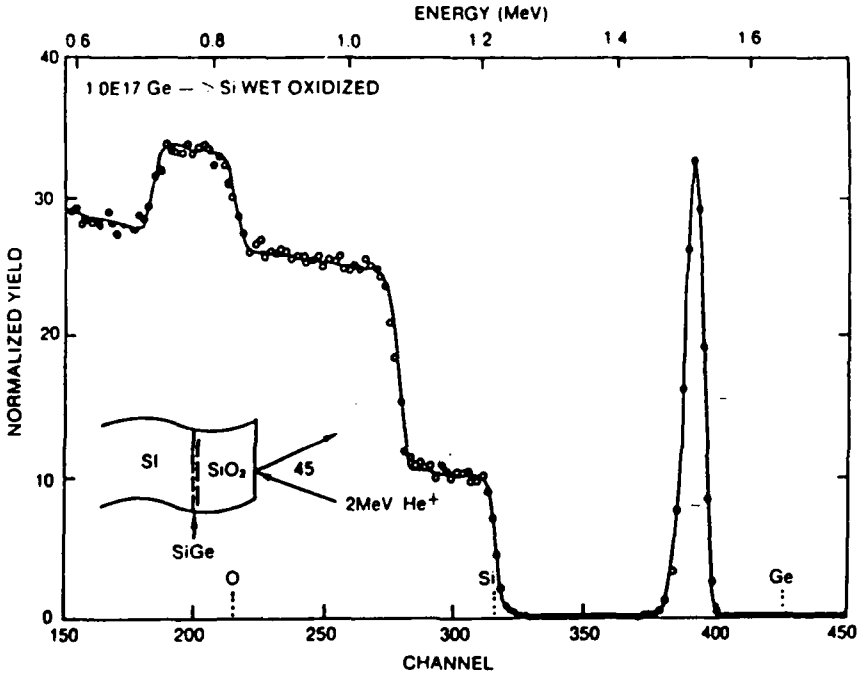


Figure 1. Rutherford backscattering spectrum of $1x10^{17}$ Ge/cm$^2$ implanted sample after wet oxidation at 900°C. Solid line shows the fit to the data using the Cornell RUMP simulation program [11].

The amount of alloying in these thin $Si_{1-x}Ge_x$ was also determined by the use of two optical techniques. The alloy concentration was found to be $Si_{0.35}Ge_{0.65}$, from the Raman Si-Ge peak position [10] and using the results of Feldman et al. [12]. This is in good agreement with the RBS data.

Electroreflectance (ER) has also been used to obtain x, the Ge concentration [10]. From the ER data and the results of Kline et al. [13], a concentration of $Si_{0.33}Ge_{0.67}$ has been determined [10].

Thus, the alloy layers contain $Si_{0.35}Ge_{0.65}$, and appear about 300Å thick. According to the results of Pearsall et al. [14], these layers should be incommensurate with the Si substrate, and should not be strained.

## MBE GROWTH OF GaAs ON SiGe SUBSTRATE

The substrates, formed by implantation and wet oxidation, were stripped of the 2400Å $SiO_2$ layer using a 10:1 solution of HF:DI (de-ionized water). They were then rinsed in DI and oxidized by the Shiroki technique using a solution of $HCl:H_2O_2:DI$ (3:1:1) at 85°C for 5 minutes. The final step involved rinsing in DI and blow drying in $N_2$. The samples were immediately loaded into a VG GaAs MBE system, using indium-free sapphire-backed holders. The base pressure prior to deposition was $2x10^{-10}$ torr.

Desorption was carried out at 600°C for 10 minutes, followed by flash heating to 650°C for 1 minute. The resulting RHEED pattern was bright and streaked, exhibiting a (2x1) reconstruction. Growth was then initiated, following the standard two-step growth process. A 300Å GaAs buffer layer was deposited at 325°C, at a rate of 0.2μm/hr. The temperature was then raised to 550°C, and a 1.25μm GaAs layer was deposited at a rate of 1μm/hr. During growth, the As to Ga pressure ratio was held at 20.

In addition, samples of GaAs grown directly on Si were also prepared under similar conditions. However, the Si substrate desorption temperature was higher, about 850°C.

## RESULTS AND DISCUSSION

Samples grown with and without the SiGe buffer layer were then analyzed using Auger spectroscopy (AES), scanning electron microscopy (SEM), and cross-sectional transmission electron microscopy (XTEM).

The Auger profiles for a) GaAs/Si and b) GaAs/SiGe/Si are shown in Figures 2a and 2b. A SiGe buffer layer is present between the GaAs and Si in Figure 2b, and it is roughly 300Å thick, with a tailing of the Ge concentration toward the silicon substrate.

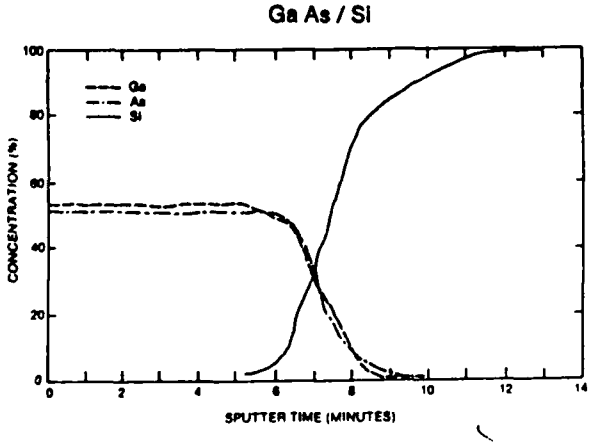


Figure 2a. Auger spectra for GaAs/Si.

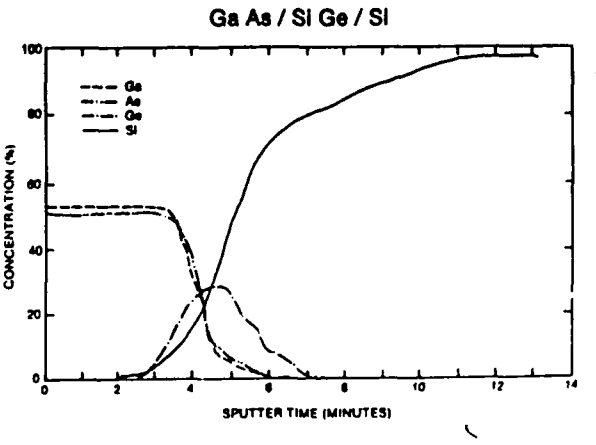


Figure 2b. Auger spectra for GaAs/SiGe/Si.

The samples grown on the SiGe buffer appeared optically smooth with a mirror-like surface, while those grown directly on Si appeared milky. The surface quality has also been examined by SEM, and the results are shown in Figure 3. Clearly, the surface of the sample using the SiGe buffer layer is smoother on a 1μm scale. It appears that either fewer defects propagate to the surface, or fewer defects are created due to the better lattice match and closer thermal expansion coefficients of GaAs and Ge.

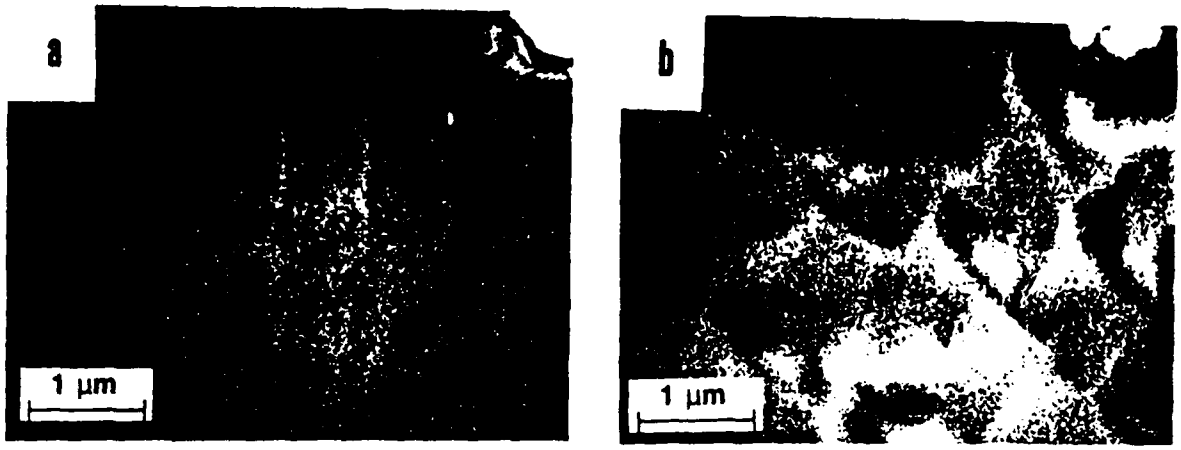


Figure 3. Scanning electron micrographs of a) GaAs/SiGe/Si and b) GaAs/Si.

Further defect characterization was carried out by XTEM. A cross-sectional micrograph of a GaAs layer grown on the SiGe is shown in Figure 4. Stacking faults, micro-twins, and dislocations can be seen, but there are areas relatively free of defects. The results in Figure 5 show the cross-section of a GaAs grown directly on Si. A higher density of defects is visible, especially threading and misfit dislocations. Clearly the samples grown on the SiGe buffer exhibit fewer defects. It should also be pointed out that these films are quite thin, on the order of 1µm, and thus exhibit higher defect concentrations due to the proximity of the interface.

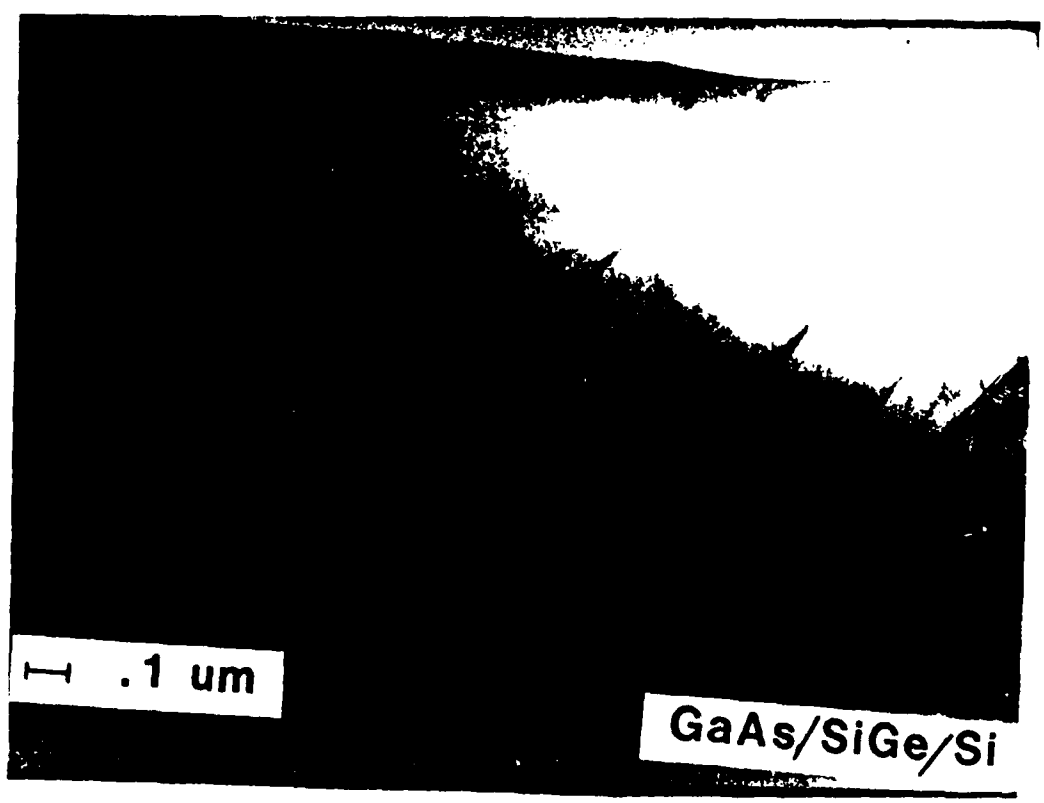


Figure 4. Cross-sectional TEM micrographs of GaAs/SiGe/Si showing twins, stacking faults, and dislocations.

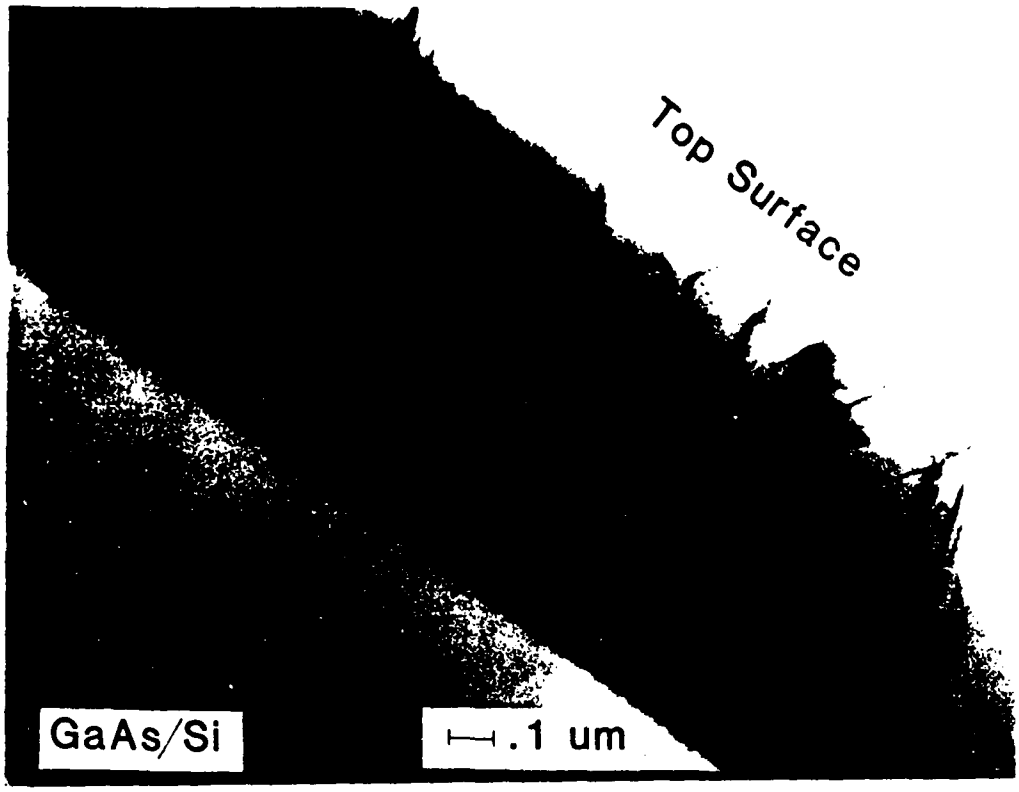


Figure 5. Cross-sectional TEM micrograph of GaAs/Si showing high density of dislocations and stacking faults.

## CONCLUSION

The effect of a SiGe buffer layer has been examined in the heteroepitaxial growth of GaAs on Si. The epitaxial SiGe buffer layers have been prepared by a novel technique of germanium implantation followed by a wet oxidation process, requiring no UHV deposition process. These layers have been characterized by RBS, Raman, and ER, and were found to be about 300Å thick, of composition $Si_{0.35}Ge_{0.65}$.

A standard two-step MBE growth of GaAs was then used to deposit GaAs on the $Si_{0.35}Ge_{0.65}$ buffer and on a Si substrate. The Ge-rich layer is present at the GaAs/Si interface, and from the results of SEM and XTEM, it appears that this layer reduces the defects which form at the initial GaAs interface, and thus can lead to higher quality material.

## ACKNOWLEDGEMENTS

We would like to thank A. Georgakilas for help in the MBE growth process, and W.E. Carlos, R. Stahlbush, and O. Glembocki for helpful discussions.

## REFERENCES

1. J.S. Harris, Jr., S.M. Koch, and S.J. Rosrner, Materials Research Society Proceedings, 91 (1987) 3.

2. H. Kroemer, J. Cryst. Growth 81 (1987) 193.

3. R.J. Fischer, N.C. Chand, W.F. Knopp, H. Morkoc, L.P. Erickson, and R. Youngman, Appl. Phys. Lett. 47 (1985) 397.

4. G.M. Metze, H.K. Choi, and B.Y. Tsaur, Appl. Phys. Lett. 45 (1984) 1107.

5. R. Fischer, H. Morkoc, D. A. Neumann, H. Zabel, C. Choi, N. Otsuka, M. Longerbone, and L.P. Erickson, J. Appl. Phys. 60 (1986) 1640.

6. D.L. Miller and J.S. Harris, Jr., Appl. Phys. Lett. 37 (1980) 1104.

7. P.R. Pukite and P.I. Cohen, J. Cryst. Growth 81 (1987) 214.

8. B.Y. Tsaur, J.C.C. Fan, and R.P. Gale, Appl. Phys. Lett. 38 (1981) 779.

9. D. Fathy, O.W. Holland, and C.W. White, Appl. Phys. Lett. 51 (1987) 1337.

10. S.M. Prokes, O.J. Glembocki, E.P. Donovan, R. Stahlbush, W.E. Carlos, H. Dietrich, and A. Christou, SPIE Proceedings, Newport Beach, CA (1988) to be published.

11. L.R. Doolittle, Nucl. Instr. and Meth. B9 (1983) 344.

12. D.W. Feldman, M. Ashkin, and J.H. Parker, Jr., Phys. Rev. Lett. 17 (1966) 1209.

13. J.S. Kline, F.H. Pollak, and M. Cardona, Helvetica Physica Acta 41 (1968) 968.

14. T.P. Pearsall, F.H. Pollak, J.C. Bean, and R. Hull, Phys. Rev B33 (1989) 33.